

## Supporting Information

A selective “turn-on” sensor for recognizing of  $\text{In}^{3+}$  and  $\text{Zn}^{2+}$  in respective system based on imidazo[2,1-*b*]thiazole

Yuankang Xu<sup>a</sup>, Songfang Zhao<sup>b,\*</sup>, Yanxia Zhang<sup>a</sup>, Hanyu Wang<sup>a</sup>,  
Xiaofeng Yang<sup>a</sup>, Meishan Pei<sup>a</sup>, Guangyou Zhang<sup>a,\*</sup>

<sup>a</sup> School of chemistry and chemical engineering, University of Jinan,  
Jinan 250022, China.

<sup>b</sup> Henan Sanmenxia Aoke Chemical Industry Co. Ltd., Sanmenxia 472000,  
China.

\*Corresponding author:

Guangyou Zhang, Ph.D, Professor, E-mail address:  
[chm\\_zhanggy@ujn.edu.cn](mailto:chm_zhanggy@ujn.edu.cn).

Songfang Zhao, E-mail address: [songfang2008@163.com](mailto:songfang2008@163.com).

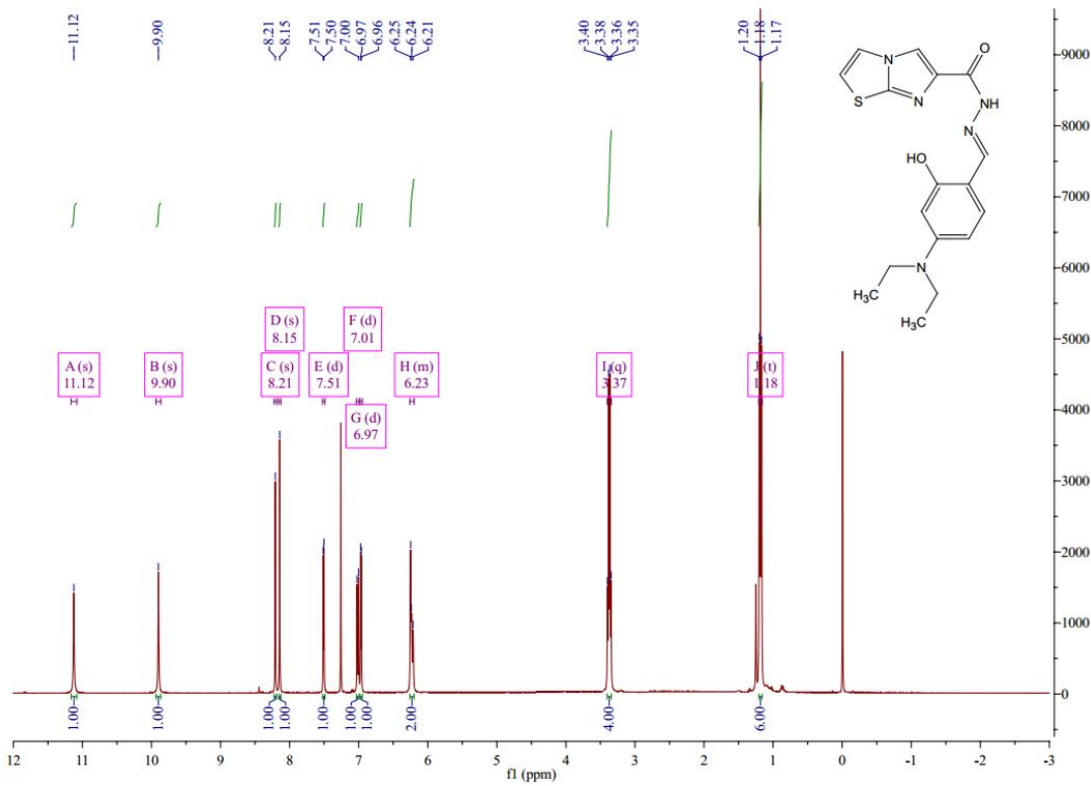


Fig. S1.  $^1\text{H}$  NMR spectrum of **X**.

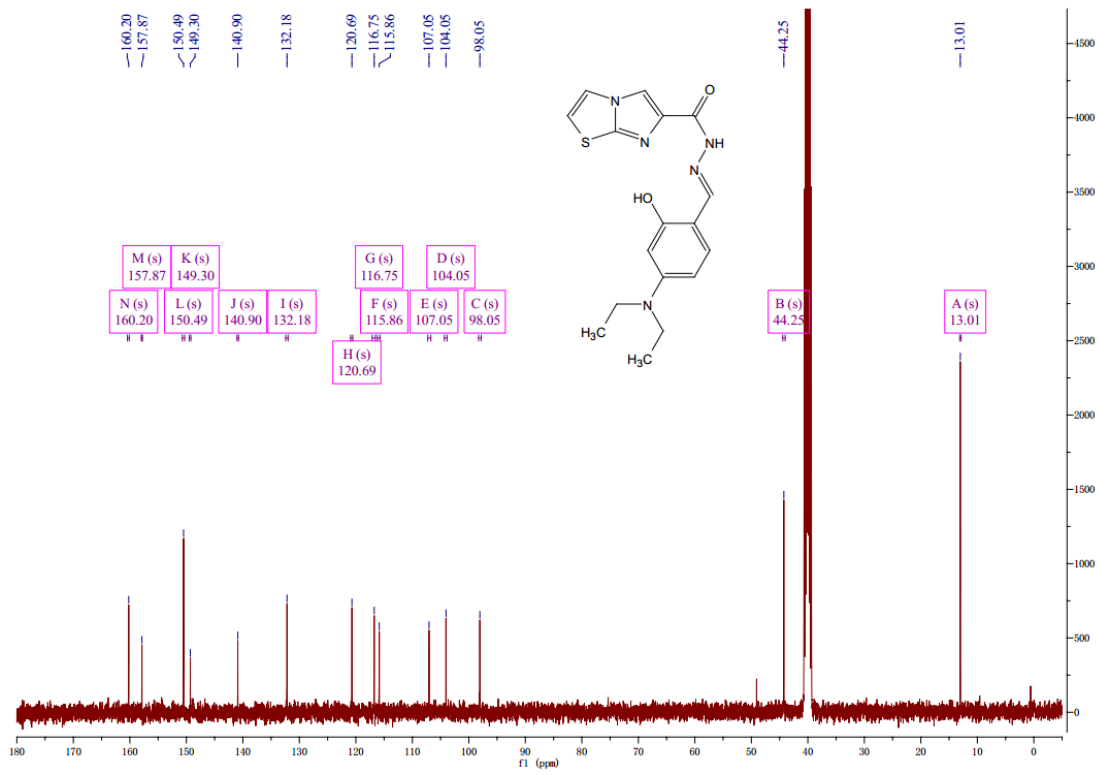


Fig. S2.  $^{13}\text{C}$  NMR spectrum of **X**.

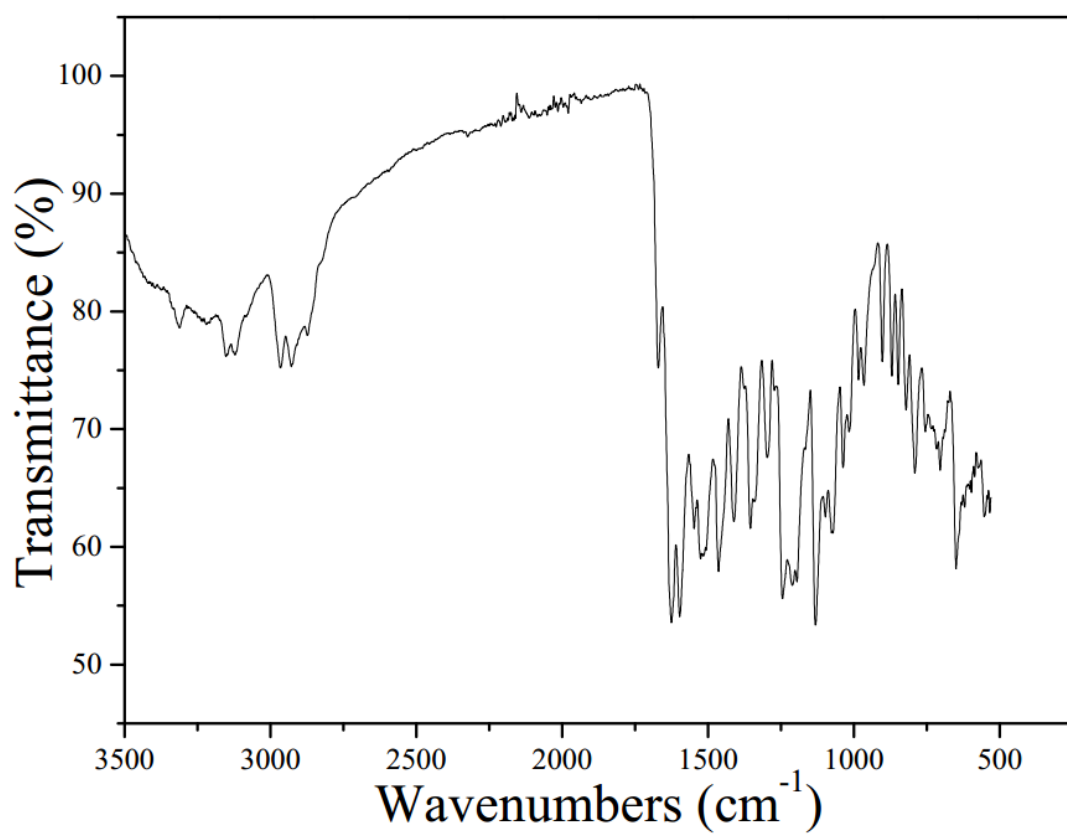


Fig. S3. The FTIR spectra of **X**.

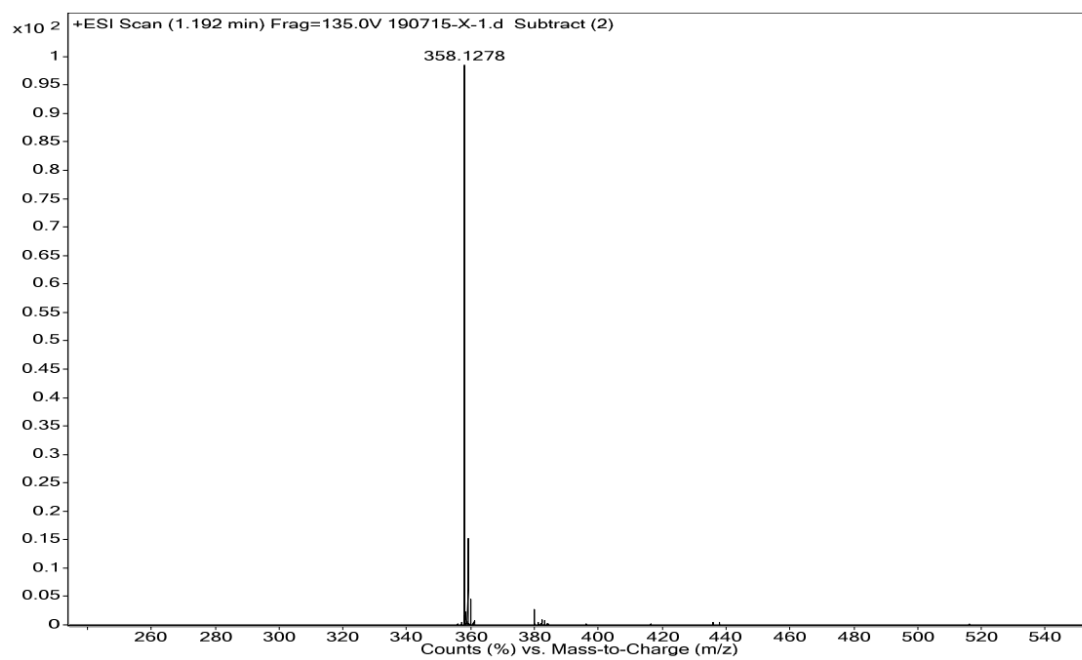


Fig. S4. ESI mass spectrum of **X**.

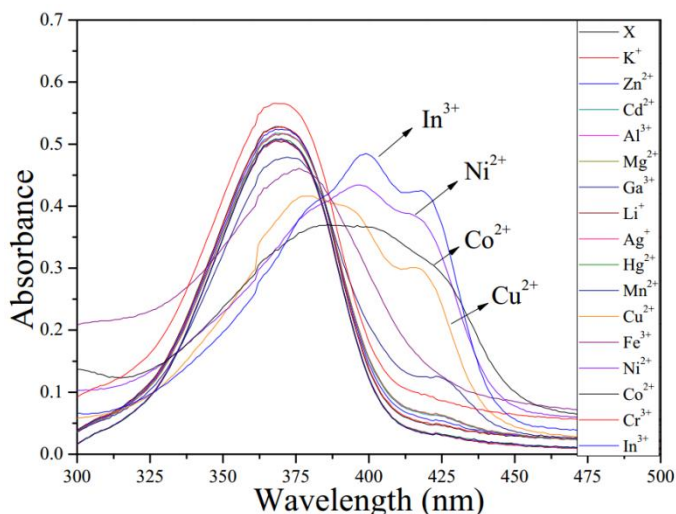


Fig. S5. Absorption spectra of **X** ( $1 \times 10^{-5}$  M) upon the addition of various metal ions (7.5 equiv.) in DMF/H<sub>2</sub>O buffer solution (v/v = 9:1, tris = 10 mM, pH = 7.4).

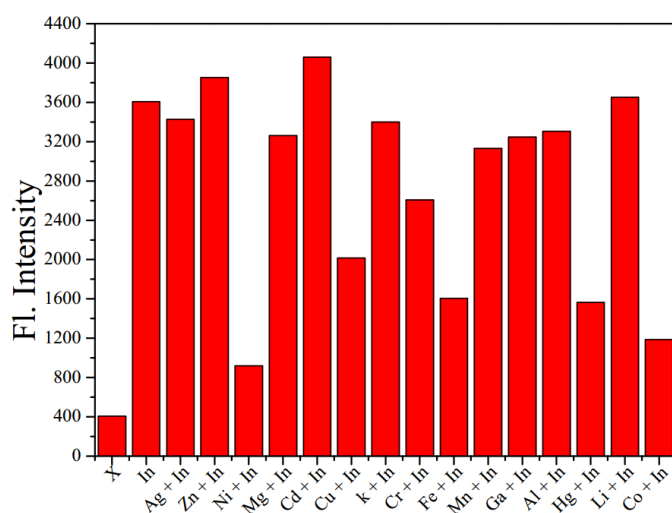


Fig. S6. Fluorescence intensity of **X** and its complexation with In<sup>3+</sup> in the presence of other metal ions (Ag<sup>+</sup>, Zn<sup>2+</sup>, Ni<sup>2+</sup>, Mg<sup>2+</sup>, Cd<sup>2+</sup>, Cu<sup>2+</sup>, K<sup>+</sup>, Cr<sup>3+</sup>, Fe<sup>3+</sup>, Mn<sup>2+</sup>, Ga<sup>3+</sup>, Al<sup>3+</sup>, Hg<sup>2+</sup>, Li<sup>+</sup> and Co<sup>2+</sup>) in DMF/H<sub>2</sub>O buffer solution (v/v = 9:1, tris = 10 mM, pH = 7.4).

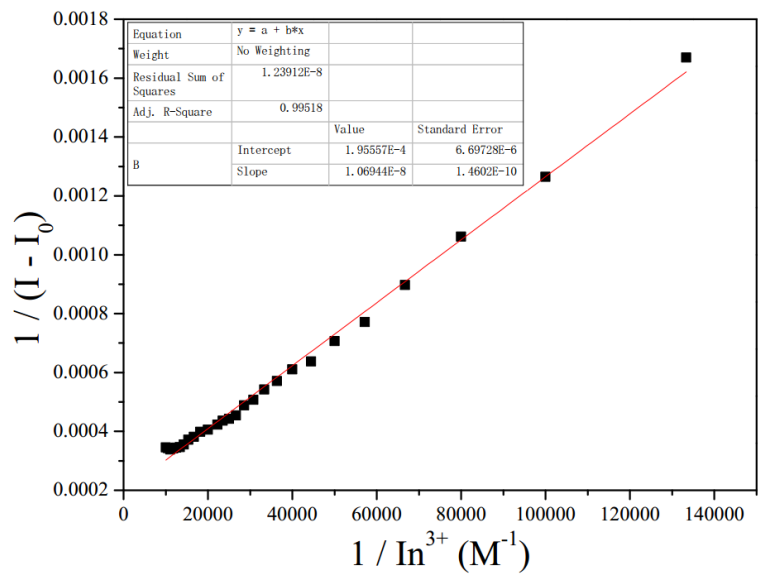


Fig. S7. Benesi-Hilderbrand plot of **X** with  $\text{In}^{3+}$ .

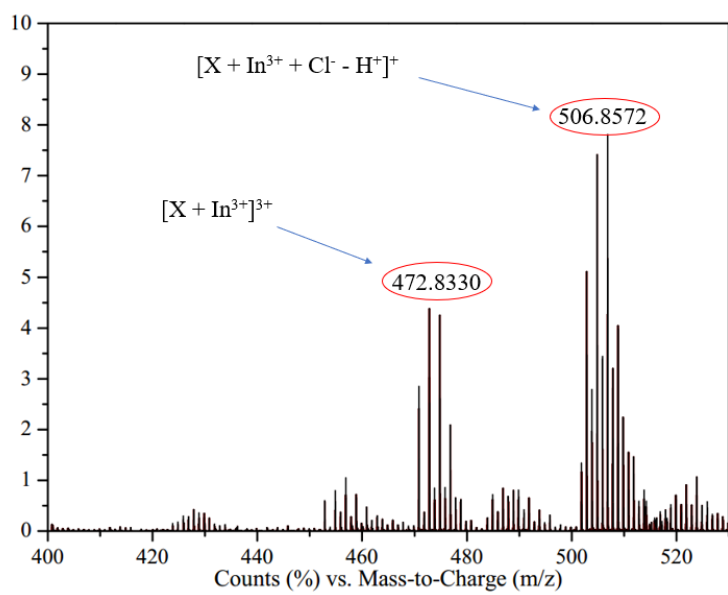


Fig. S8. ESI Mass spectrum of **X**[ $\text{In}^{3+}$ ].

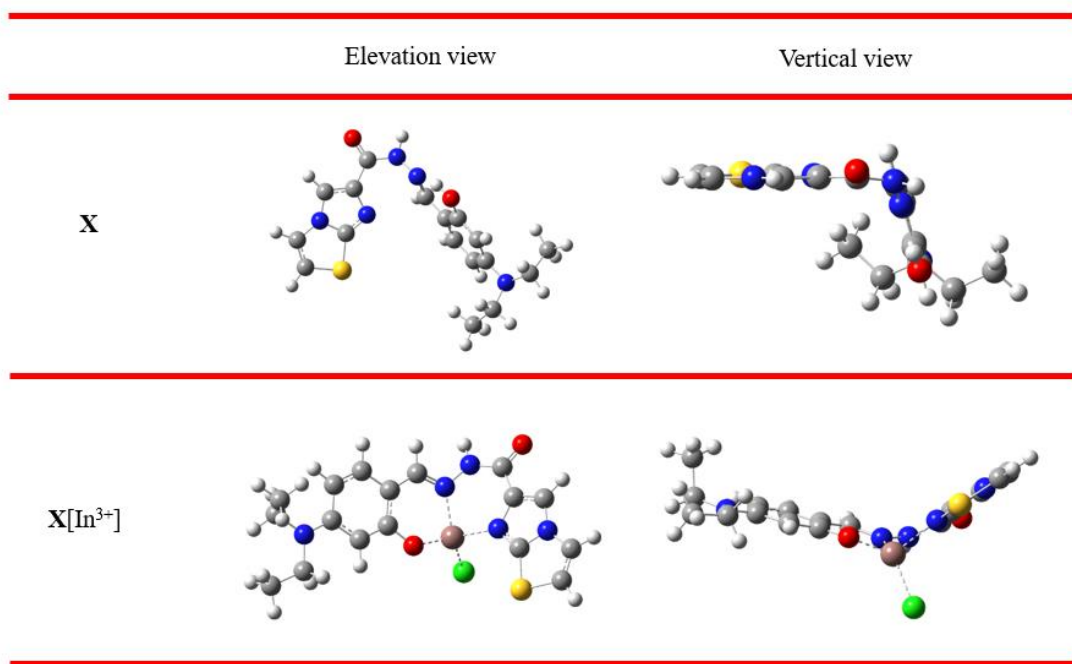


Figure S9. The optimized geometry of **X** and **X**[In<sup>3+</sup>] at the B3LYP level of theory, where the light-gray, red, blue, white, brown and cyan spheres denote C, O, N, H, In and Cl atoms, respectively.

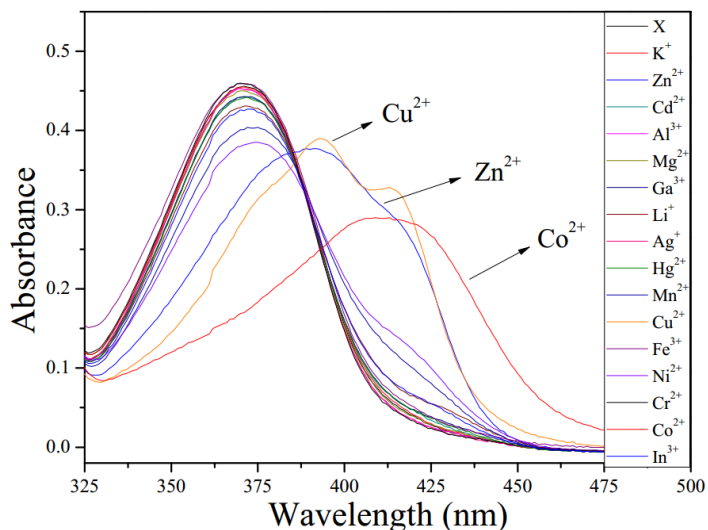


Fig. S10. Absorption spectra of **X** ( $1 \times 10^{-5}$  M) upon the addition of various metal ions (7.5 equiv.) in EtOH/H<sub>2</sub>O buffer solution (v/v = 9:1, tris = 10 mM, pH = 7.4).

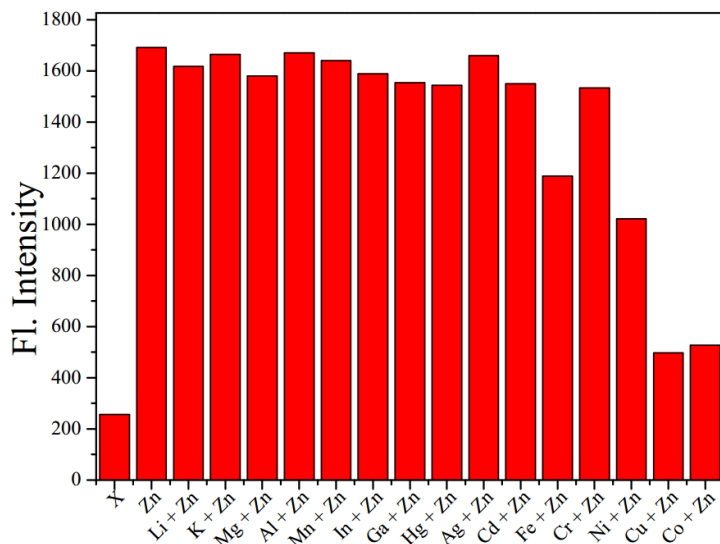


Fig. S11. Fluorescence intensity of **X** and its complexation with Zn<sup>2+</sup> in the presence of other metal ions (Li<sup>+</sup>, K<sup>+</sup>, Mg<sup>2+</sup>, Al<sup>3+</sup>, Mn<sup>2+</sup>, In<sup>3+</sup>, Ga<sup>3+</sup>, Hg<sup>2+</sup>, Ag<sup>+</sup>, Cd<sup>2+</sup>, Fe<sup>3+</sup>, Cr<sup>3+</sup>, Ni<sup>2+</sup>, Cu<sup>2+</sup> and Co<sup>2+</sup>) in EtOH/H<sub>2</sub>O buffer solution (v/v = 9:1, tris = 10 mM, pH = 7.4).

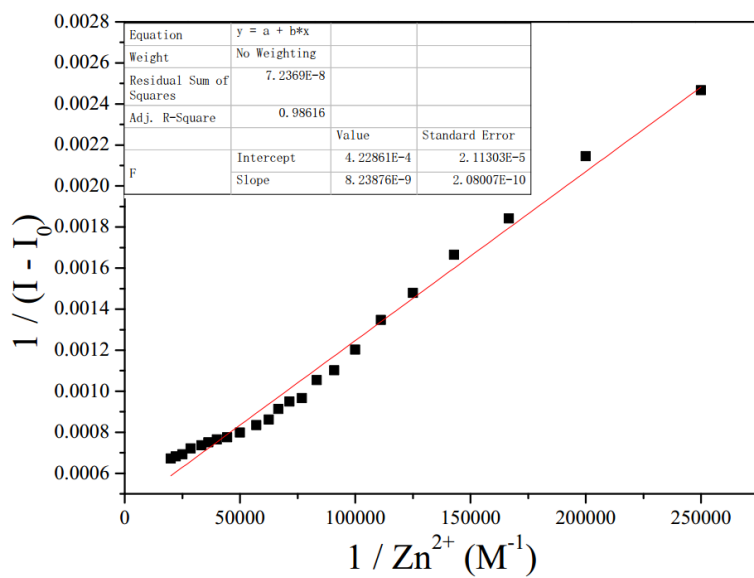


Fig. S12. Benesi-Hilderbrand plot of **X** with Zn<sup>2+</sup>.

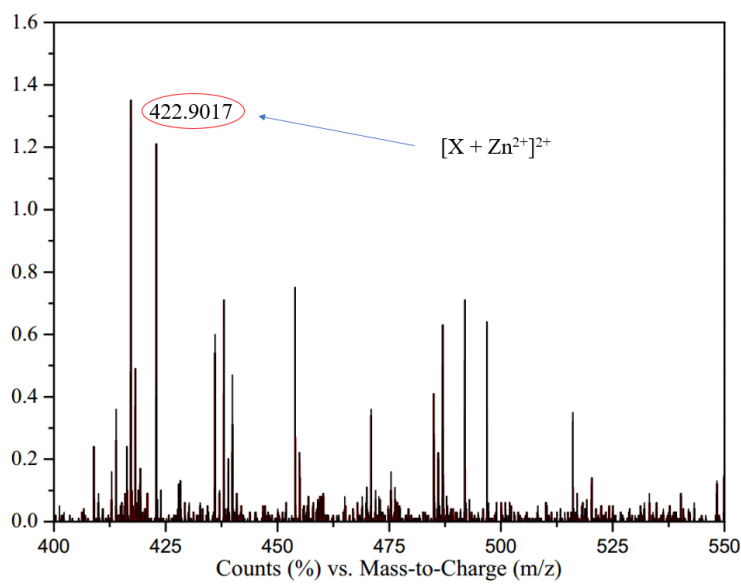


Fig. S13. ESI Mass spectrum of  $\mathbf{X}[\text{Zn}^{2+}]$ .

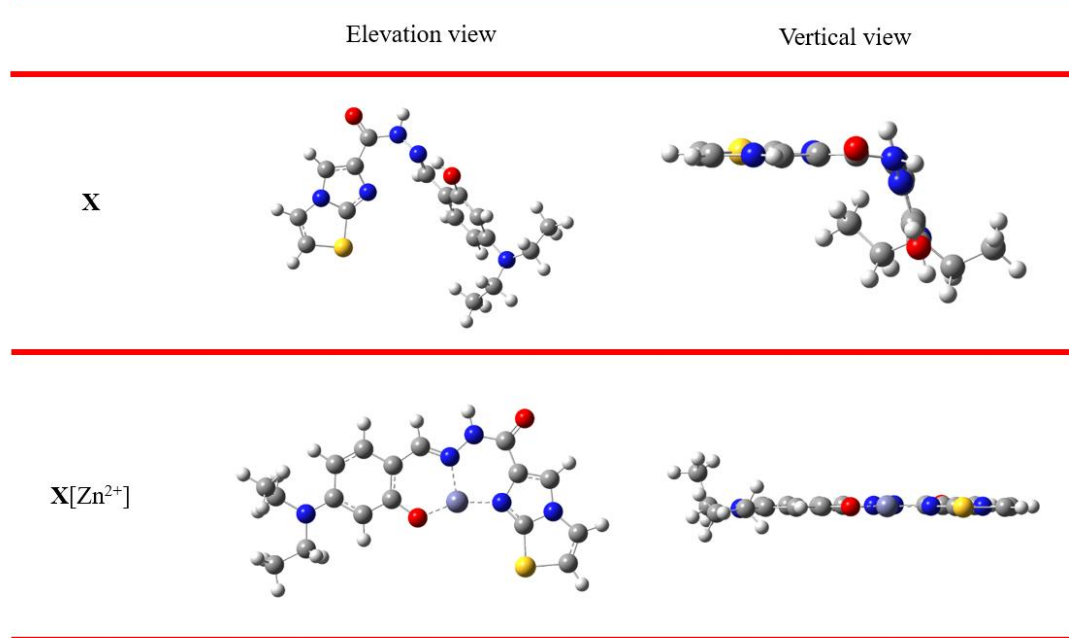
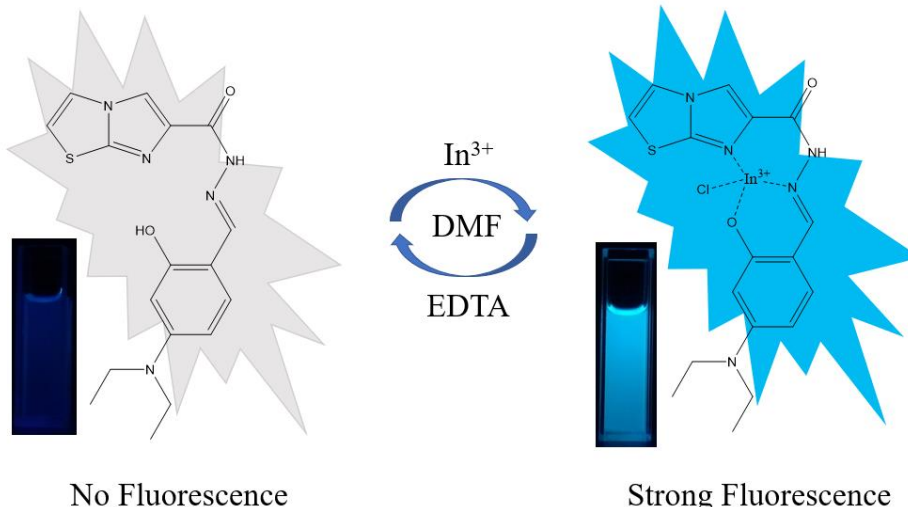
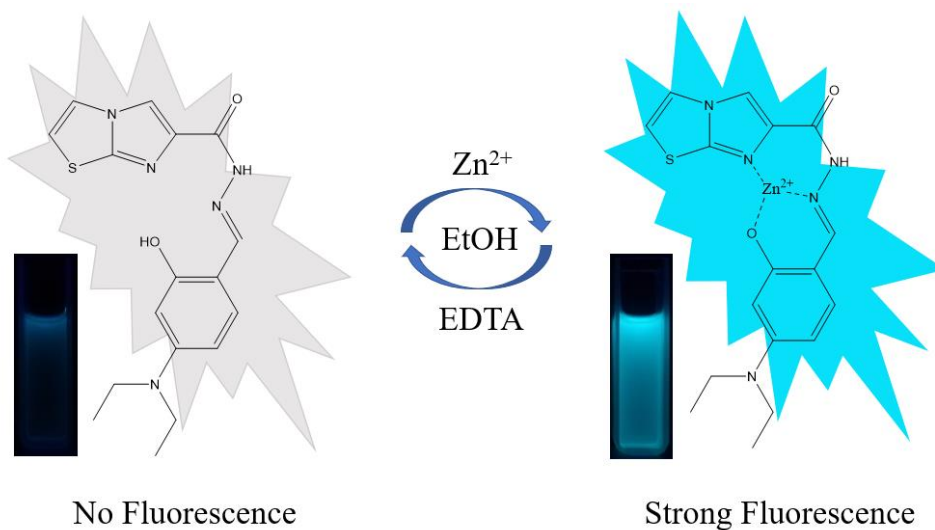


Figure S14. The optimized geometry of  $\mathbf{X}$  and  $\mathbf{X}[\text{Zn}^{2+}]$  at the B3LYP level of theory, where the light-gray, red, blue, white, dark-gray and cyan spheres denote C, O, N, H, Zn and Cl atoms, respectively.



Scheme 2. The proposed binding mode of **X** with  $\text{In}^{3+}$ .



Scheme 3. The proposed binding mode of **X** with  $\text{Zn}^{2+}$ .

Table S1. Comparative study of the analytical performance of **X** with other previous sensors.

sensor	Reaction media	Target ion	LOD (M)	$K_a$	Ref.
1	DMF/H <sub>2</sub> O (v/v = 9/1)	$\text{In}^{3+}$	$1.02 \times 10^{-9}$	$1.01 \times 10^5 \text{ M}^{-1}$	This work
2	MeOH	$\text{In}^{3+}$	$7.9 \times 10^{-6}$	$1.0 \times 10^8 \text{ M}^{-2}$	[17]
3	EtOH	$\text{In}^{3+}$	$6.1 \times 10^{-7}$	$8.1 \times 10^4 \text{ M}^{-2}$	[21]
4	MeOH	$\text{In}^{3+}$	$2.0 \times 10^{-6}$	$1.4 \times 10^5 \text{ M}^{-1}$	[22]
5	DMF	$\text{In}^{3+}$	$5.0 \times 10^{-8}$	$2.0 \times 10^{10} \text{ M}^{-2}$	[23]
6	EtOH/H <sub>2</sub> O (v/v = 9/1)	$\text{Zn}^{2+}$	$5.5 \times 10^{-9}$	$2.65 \times 10^5 \text{ M}^{-1}$	This work
7	EtOH/H <sub>2</sub> O (v/v = 9/1)	$\text{Zn}^{2+}$	$2.86 \times 10^{-7}$	$1.81 \times 10^5 \text{ M}^{-1}$	[25]
8	MeOH/H <sub>2</sub> O (v/v = 1/9)	$\text{Zn}^{2+}$	$7.95 \times 10^{-7}$	$6.0 \times 10^3 \text{ M}^{-1}$	[26]
9	EtOH	$\text{Zn}^{2+}$	$4.0 \times 10^{-8}$	$6.4 \times 10^4 \text{ M}^{-1}$	[27]
10	EtOH/H <sub>2</sub> O (v/v = 99/1)	$\text{Zn}^{2+}$	$5.03 \times 10^{-7}$	$85.7 \text{ M}^{-2}$	[29]

Table S2. Determination of In<sup>3+</sup> concentrations in tap water samples.

sample	In <sup>3+</sup> added (M)	In <sup>3+</sup> recovered (M)	Recovery (%)	RSD (%)
1	1.0 × 10 <sup>-5</sup>	9.28 × 10 <sup>-6</sup>	92.8	0.74
2	2.0 × 10 <sup>-5</sup>	1.88 × 10 <sup>-5</sup>	94.1	2.36
3	3.0 × 10 <sup>-5</sup>	2.74 × 10 <sup>-5</sup>	91.2	2.27
4	4.0 × 10 <sup>-5</sup>	3.68 × 10 <sup>-5</sup>	92.3	3.51

Table S3. Determination of Zn<sup>2+</sup> concentrations in tap water samples.

sample	Zn <sup>2+</sup> added (M)	Zn <sup>2+</sup> recovered (M)	Recovery (%)	RSD (%)
1	1.0 × 10 <sup>-5</sup>	9.73 × 10 <sup>-6</sup>	97.3	3.01
2	2.0 × 10 <sup>-5</sup>	2.08 × 10 <sup>-5</sup>	104.1	2.39
3	3.0 × 10 <sup>-5</sup>	3.19 × 10 <sup>-5</sup>	106.2	1.50

The specific configuration and test process

Stock solutions of the ions (In<sup>3+</sup> and Zn<sup>2+</sup>) were prepared with a concentration of 0.03 M in distilled water and tap water. The probe **X** was dissolved in ethanol/H<sub>2</sub>O (v/v = 9 : 1) buffer solution (10 mM tris, pH = 7.4) and DMF/H<sub>2</sub>O (v/v = 9 : 1) buffer solution (10 mM tris, pH = 7.4) at room temperature with the concentration of 1 × 10<sup>-5</sup> M.

The fluorescence intensity was measured when the In<sup>3+</sup> (distilled water) concentration were 1 × 10<sup>-5</sup> M, 2 × 10<sup>-5</sup> M, 3 × 10<sup>-5</sup> M and 4 × 10<sup>-5</sup> M. Then, the fluorescence intensity was measured with three times when the In<sup>3+</sup> (tap water) concentration were 1 × 10<sup>-5</sup> M, 2 × 10<sup>-5</sup> M, 3 × 10<sup>-5</sup> M and 4 × 10<sup>-5</sup> M.

For example:

Determination of In<sup>3+</sup> concentrations in tap water samples, sample 1, Table S2.

Fluorescence intensity: 751.3 (distilled water, 1 × 10<sup>-5</sup> M); 1281 (distilled water, 2 × 10<sup>-5</sup> M);

1829 (distilled water, 3 × 10<sup>-5</sup> M); 2639 (distilled water, 4 × 10<sup>-5</sup> M).

Linear equation: Y = 621.1X + 72.3

Fluorescence intensity (three times): 645.8 (tap water, 1 × 10<sup>-5</sup> M); 654.5 (tap water, 1 × 10<sup>-5</sup> M);

646.7 (tap water, 1 × 10<sup>-5</sup> M).

The average of fluorescence intensity: (645.8 + 654.5 + 646.7) / 3 = 649

In<sup>3+</sup> recovered (M) = (649 - 72.3) / 621.1 = 0.928; 9.28 × 10<sup>-6</sup> M

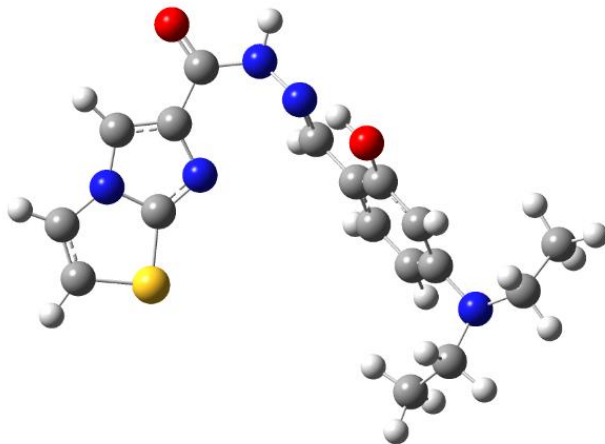
Recovery = In<sup>3+</sup> recovered (M) / In<sup>3+</sup> added (M) = 9.28 × 10<sup>-6</sup> / 1.0 × 10<sup>-5</sup> = 92.8%

according to formula  $\sigma = \sqrt{\frac{1}{n-1} \sum_{i=1}^n (x_i - \bar{x})^2}$ . The standard deviation ( $\sigma$ ) was calculated to be 4.78.

RSD =  $\sigma / \bar{x} = 4.78 / 649 = 0.0073, 0.73\%$

The calculation of other data was similar to the example.

Table S4. XYZ coordinate of the optimized structure of **X**.



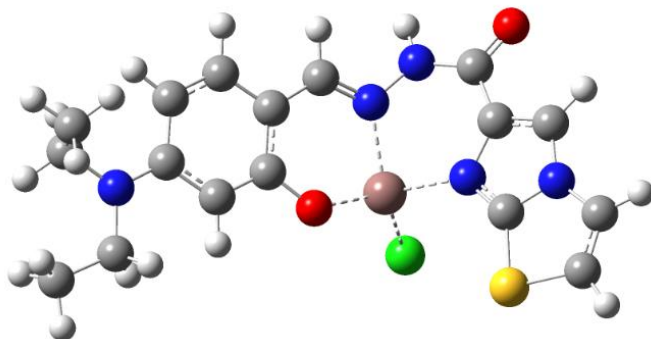
Standard orientation:

Center Number	Atomic Number	Atomic Type	Coordinates (Angstroms)		
			X	Y	Z
1	6	0	-5.286854	-1.689122	1.297058
2	6	0	-5.029600	-2.846596	0.505276
3	6	0	-4.245195	-0.756948	-0.580441
4	6	0	-4.389607	0.673399	1.158164
5	6	0	-3.481765	1.171424	0.203984
6	6	0	-2.663186	2.468481	0.342442
7	6	0	-0.170494	1.159687	-0.955533
8	7	0	-5.104271	-0.432312	0.532110
9	7	0	-3.424538	0.236037	-0.949725
10	16	0	-4.468550	-2.408646	-1.132110
11	8	0	-2.785476	3.182897	1.371143
12	7	0	-1.738967	2.872038	-0.727071
13	7	0	-0.473979	2.324584	-0.481918
14	6	0	1.220999	0.557498	-0.685874
15	6	0	2.251201	1.342095	0.147609
16	6	0	3.517459	0.794103	0.393001
17	6	0	3.878749	-0.592685	-0.170817
18	6	0	2.941266	-1.306666	-0.929288
19	6	0	1.549775	-0.704476	-1.198952
20	6	0	5.168273	-1.954254	1.327734
21	6	0	4.136916	-3.088863	1.184332
22	6	0	6.191465	-0.084469	0.223477
23	6	0	6.232026	0.739741	-1.076766
24	7	0	5.206989	-1.167506	0.086594
25	1	0	-5.139788	-3.851755	0.855155
26	1	0	-5.567763	-1.723522	2.328953

27	1	0	-4.525303	1.034849	2.156081
28	1	0	-1.671631	3.869490	-0.750669
29	1	0	-0.886282	0.614548	-1.534645
30	1	0	0.833986	-1.249617	-1.778061
31	1	0	3.192291	-2.270214	-1.321031
32	1	0	4.233248	1.339245	0.972109
33	8	0	1.915715	2.629823	0.671161
34	1	0	1.286207	3.058720	0.086895
35	1	0	6.135086	-2.372664	1.515100
36	1	0	4.889872	-1.320179	2.143419
37	1	0	4.415317	-3.722938	0.368648
38	1	0	4.108734	-3.661530	2.087747
39	1	0	3.170103	-2.670453	0.996965
40	1	0	5.913062	0.549607	1.039161
41	1	0	7.158278	-0.502878	0.410846
42	1	0	5.265214	1.158150	-1.264135
43	1	0	6.948618	1.528073	-0.977130
44	1	0	6.510429	0.105664	-1.892449

---

Table S5. XYZ coordinate of the optimized structure of  $\mathbf{X}[\text{In}^{3+}]$ .



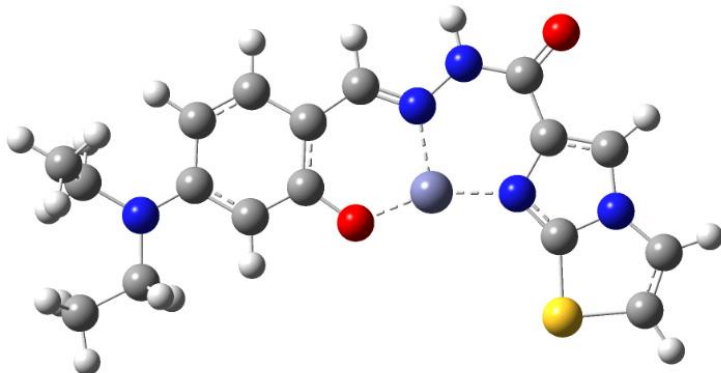
Standard orientation:

Center Number	Atomic Number	Atomic Type	Coordinates (Angstroms)		
			X	Y	Z
1	6	0	6.237351	-1.111169	0.104403
2	6	0	5.900047	-2.426783	0.124242
3	6	0	3.896381	-0.931753	0.055332
4	6	0	4.868171	1.105480	0.034367
5	6	0	3.500757	1.284462	0.004894
6	6	0	2.903405	2.663629	-0.033401
7	6	0	-0.789116	2.335051	-0.091511
8	6	0	-1.942531	1.527127	-0.101003
9	6	0	-2.020264	0.068346	-0.081086
10	6	0	-3.222850	-0.603361	-0.101810
11	6	0	-4.482661	0.101076	-0.151119
12	6	0	-4.421182	1.551995	-0.150763
13	6	0	-3.219212	2.210667	-0.131842
14	6	0	-5.659692	-2.073075	-0.150488
15	6	0	-7.026258	-2.752283	-0.304698
16	6	0	-6.964891	0.166868	-0.206641
17	6	0	-7.431265	0.579927	1.205484
18	16	0	4.091018	-2.700452	0.094673
19	7	0	5.100695	-0.271469	0.065571
20	7	0	2.875737	-0.026013	0.018259
21	8	0	3.690119	3.636644	-0.037985
22	7	0	1.535062	2.891704	-0.063755
23	7	0	0.514107	1.916691	-0.063674
24	8	0	-0.865739	-0.733998	-0.038136
25	7	0	-5.661859	-0.566500	-0.199356
26	1	0	7.233658	-0.690920	0.115299
27	1	0	6.553045	-3.286981	0.154006
28	1	0	5.643360	1.855868	0.034547
29	1	0	1.262980	3.875027	-0.089442

30	1	0	-0. 949078	3. 413696	-0. 109409
31	1	0	-3. 218664	3. 298314	-0. 137236
32	1	0	-5. 330721	2. 136961	-0. 162299
33	1	0	-3. 180573	-1. 683605	-0. 078735
34	1	0	-6. 876238	1. 037514	-0. 863373
35	1	0	-7. 708629	-0. 483521	-0. 665282
36	1	0	-8. 394498	1. 098208	1. 133471
37	1	0	-7. 568971	-0. 294818	1. 850892
38	1	0	-6. 718374	1. 254515	1. 693799
39	1	0	-5. 003830	-2. 429263	-0. 955475
40	1	0	-5. 212206	-2. 376778	0. 806522
41	1	0	-7. 481847	-2. 562035	-1. 282480
42	1	0	-6. 869616	-3. 834523	-0. 226820
43	1	0	-7. 733792	-2. 471010	0. 482004
44	49	0	0. 878608	-0. 049515	-0. 021454
45	17	0	1. 126325	-1. 484262	0. 000000

---

Table S6. XYZ coordinate of the optimized structure of  $\mathbf{X}[\text{Zn}^{2+}]$ .



Standard orientation:

Center Number	Atomic Number	Atomic Type	Coordinates (Angstroms)		
			X	Y	Z
1	6	0	9.155514	-0.587574	-0.124890
2	6	0	9.502229	-2.358469	-0.107720
3	6	0	6.794288	-1.235770	-0.019087
4	6	0	6.525207	1.863029	-0.062636
5	6	0	5.087452	1.654306	-0.099225
6	6	0	3.445473	2.971061	-0.044245
7	6	0	-1.469868	3.072750	0.133254
8	6	0	-2.893709	1.329677	0.246067
9	6	0	-3.163982	-0.879914	0.332556
10	6	0	-5.163436	-1.201640	-0.003338
11	6	0	-6.499834	-0.246889	-0.115617
12	6	0	-6.543304	1.519982	-0.271853
13	6	0	-5.166845	2.256026	-0.307351
14	6	0	-7.716503	-2.790149	0.082132
15	6	0	-8.996326	-3.450589	-0.463278
16	6	0	-9.164387	0.955448	-0.277837
17	6	0	-10.463495	0.713459	0.512959
18	16	0	7.828092	-2.724789	-0.034339
19	7	0	7.726180	0.255221	-0.082492
20	7	0	4.856363	-0.518551	0.024669
21	8	0	4.082139	4.054808	-0.105230
22	7	0	2.007828	3.274832	-0.001821
23	7	0	0.251040	1.931793	0.109397
24	8	0	-2.002454	-1.705925	0.216551
25	7	0	-7.864524	-0.792929	-0.096571
26	1	0	10.028048	0.030078	-0.170614
27	1	0	10.396130	-2.945999	-0.133176
28	1	0	6.934056	2.851157	-0.025955

29	1	0	1. 786589	4. 249715	-0. 027442
30	1	0	-1. 630609	4. 130162	0. 102547
31	1	0	-5. 193490	3. 283629	-0. 604372
32	1	0	-7. 467604	2. 054893	-0. 338483
33	1	0	-5. 391706	-2. 238347	-0. 137622
34	1	0	-8. 662701	1. 815119	0. 114816
35	1	0	-9. 399652	1. 119639	-1. 308658
36	1	0	-11. 289730	1. 134303	-0. 021012
37	1	0	-10. 616179	-0. 338561	0. 634781
38	1	0	-10. 387203	1. 176500	1. 474558
39	1	0	-6. 871192	-3. 136420	-0. 475046
40	1	0	-7. 593813	-3. 047852	1. 113362
41	1	0	-9. 626228	-2. 702738	-0. 897838
42	1	0	-8. 735217	-4. 173512	-1. 207660
43	1	0	-9. 516760	-3. 934393	0. 336710
44	30	0	1. 763375	-0. 836095	0. 169945

---

The calculation process of detection limit:

Scan the blank sample solution 10 times and calculate the standard deviation ( $\sigma$ ) according to formula  $\sigma = \sqrt{\frac{1}{n-1} \sum_{i=1}^n (x_i - \bar{x})^2}$ . The standard deviation ( $\sigma$ ) was calculated to be 0.48.

The fluorescence emission spectra were measured when the  $Zn^{2+}$  concentration were  $1 \times 10^{-7}$  M,  $2 \times 10^{-7}$  M,  $3 \times 10^{-7}$  M,  $4 \times 10^{-7}$  M,  $5 \times 10^{-7}$  M and  $6 \times 10^{-7}$  M, respectively. As shown in Fig 9 (b) inset, a good linear relationship ( $R^2 = 0.9858$ ) between the fluorescence intensity at 463 nm and concentration of  $Zn^{2+}$  was obtained.

The slope of the line is  $26 \times 10^7$  M. based on  $3\sigma/s$  equation,  $LOD = \frac{3 \times 0.48}{26 \times 10^7} = 5.5 \times 10^{-9}$  M.